

Simulations of H₂O₂ concentration profiles in the water surrounding spent nuclear fuel taking mixed radiation fields and bulk reactions into account

Fredrik Nielsen, Mats Jonsson *

KTH Chemical Science and Engineering, Nuclear Chemistry, Royal Institute of Technology, SE, 100 44 Stockholm, Sweden

Received 30 March 2007; accepted 28 August 2007

Abstract

To simulate the dynamics of the concentration gradient of hydrogen peroxide in groundwater surrounding spent nuclear fuel under various conditions, a model has been developed. The model treats the water volume as a sequence of volume elements, and applies the processes that affect hydrogen peroxide concentration to each volume element. The surface steady-state concentrations of H₂O₂, and the time to reach steady-state, have been determined under different conditions. The processes accounted for in the model are radiolytic production of H₂O₂ from α - and β -radiation, surface reactions consuming H₂O₂, homogeneous reactions consuming H₂O₂, and diffusion. The system has been modeled mainly for different surface reaction rate constants and homogeneous (bulk) reaction rate constants. The simulations show that the surface concentration of H₂O₂ approaches the steady-state concentration very rapidly and that the impact of homogeneous (bulk) reactions consuming H₂O₂ on the steady-state concentration is significant.

© 2007 Elsevier B.V. All rights reserved.

1. Introduction

The limiting factor for release of radio-toxic species from a future deep geological repository for spent nuclear fuel to the environment is assumed to be the solubility of UO₂ in the water surrounding the spent fuel [1]. The environment at the depth of the deep repository is expected to have reducing conditions, under which the solubility of UO₂ in ground water is very low and the release rate is therefore also expected to be low [2]. However, reactive radical and molecular products will be produced radiolytically when spent fuel is in contact with water. Both oxidants (OH[•], H₂O₂, HO₂[•] and O₂) and reductants (e_{aq}⁻, H[•] and H₂) are produced by radiolysis of water [3]. For kinetic reasons, the oxidants produced alter the otherwise reducing conditions, and can thereby cause oxidation and dissolution of the spent nuclear fuel matrix. When carbonate is present, as in Swedish groundwater where the concentra-

tion is 2–10 mM [4], OH[•] will quantitatively be converted into CO₃^{-•}, this also being a strong oxidant ($E^{\circ} = 1.9$ V and 1.59 V vs. NHE, respectively [5,6]). In terms of surface reactivity, this will be of minor importance since the rate constants for both oxidants are limited by diffusion. Carbonate is also known to form strong soluble complexes with UO₂²⁺ [7] and thereby enhance the solubility of U(VI).

The kinetics for reactions between different oxidants and the spent fuel matrix (UO₂) has been studied quite extensively [8,9]. On the basis of these results it has been possible to assess the relative reactivity of the radiolytically formed oxidants [10]. The relative importance of the different radiolysis products has been discussed for several years. However, it should be stressed that the relative reactivity is not the same as the relative importance or impact of the reactant. The latter being the product of the reactivity (rate constant) and the surface concentration of the reactant. Very recently, it was shown that the molecular products, although in general being less reactive than some of the oxidizing radicals, have the highest impact (relative importance) for all types of radiation (except for very short

* Corresponding author. Tel.: +46 8 790 9123; fax: +46 8 7908772.

E-mail address: matsj@nuchem.kth.se (M. Jonsson).

irradiation time where the impact of radicals is significant). The rationale for this is simply that the concentration of molecular products is many orders of magnitude higher than the concentration of radical products. In a system exposed to α -radiation, the relative impact of H_2O_2 was found to be 99.9–100% [10]. Hence, the only oxidant that must be accounted for in a safety assessment of a future deep repository is H_2O_2 . At HCO_3^- concentrations higher than 1 mM the rate limiting step in the reaction between H_2O_2 and UO_2 has been shown to be oxidation while at lower concentrations dissolution of oxidized UO_2 influences the kinetics [9]. Consequently, the rate of spent fuel dissolution can be approximated by the rate of H_2O_2 consumption at the fuel surface in groundwater containing more than 1 mM HCO_3^- . The maximum rate of H_2O_2 consumption can never exceed the rate of radiolytic H_2O_2 production in the system. When the rates are equivalent the system has reached steady-state. The consumption of H_2O_2 at the surface is determined by the rate constant and the concentration of H_2O_2 . The rate constant for the reaction between H_2O_2 and UO_2 is well known [9]. However, the presence of ϵ -particles (metallic inclusions of fission products in the fuel matrix) can also influence the total rate constant for consumption of H_2O_2 at the fuel surface.

Consequently, the steady-state concentration depends on the dose rate (depending on the fuel age and burn-up) as well as on the rate constant for the surface reaction (in a system where no other reactions take place). If the time for reaching steady-state is insignificant in comparison to the total time of interest, simulation of spent fuel dissolution can be significantly simplified without loss of accuracy.

We have recently developed a model describing the geometrical α - and β -dose distribution as function of fuel age and burn-up [11]. Using this model, the dynamics for approaching steady-state in the α -region (taking into account the radiolytic production of H_2O_2 , diffusion of H_2O_2 and consumption of H_2O_2 by reaction with a UO_2 surface) has been investigated [12]. This study showed that the surface concentration of H_2O_2 reached 90% of the steady-state concentration within a very short time (minutes–hours). Ninety percent of the steady-state concentration was used as a limit since the concentration will approach steady-state asymptotically and thus never reach a true steady-state. In this work, we extend the study to involve also β -radiation. As the range for β -particles is significantly longer than for α -particles, the volume treated in this study is also larger. To describe a larger water volume, an extended model has been created. In addition, the impact of reactions between H_2O_2 and solutes on the steady-state surface concentration has been studied.

2. Methods

The model underlying the simulations is fairly simple. The system was modeled in one space dimension; the distance from the fuel surface. The volume is divided into

smaller elements, layers, and the H_2O_2 concentration for each volume element is stored in a vector. For each time-step the H_2O_2 concentration in each element is calculated taking the relevant processes into account. These processes are:

1. Radiolytic production from α - and β -radiation.
2. Diffusion.
3. Surface reaction.
4. Homogeneous reaction.

The radiolytic production of H_2O_2 is determined by the α - and β -dose rates, which in turn are determined by the composition of the spent nuclear fuel. Spent fuel with a certain age and burn-up has a specific dose rate profile, i.e. dose rate as a function of distance from the spent fuel surface. Dose rate profiles are used to calculate the rate of production as a function of distance from the surface. The production of H_2O_2 is applied to each element.

The surface reaction is accounted for only in the water layer closest to the surface. H_2O_2 consumption is determined by the surface reaction rate constant (partly depending on the surface concentration of ϵ -particles) and concentration of H_2O_2 at the surface.

Homogeneous reactions occur in the water due to the presence of H_2O_2 consuming species, such as Fe^{2+} from the cast iron insert of the fuel canister. The total amount of H_2O_2 is assumed to be very low compared to these species.

To determine the radiolytic production rate of H_2O_2 , the geometrical α - and β -dose rate distributions determined from the model mentioned above were used. The dose rates are determined based on an inventory for spent fuel at 100 years, with a burn-up of 38 MWd/kg U [11,13]. The dose rate is described as a function of distance from the surface, which must be converted into the rate of H_2O_2 production. A simple approach for converting dose rate to H_2O_2 production would have been to use the radiation chemical yield, i.e., the G -value. In order to make sure that the rate of production does not depend on H_2O_2 concentration we performed numerical simulations using MAKSIMA-CHEMIST [14]. Based on these simulations and the geometrical dose distribution a function describing the rate of H_2O_2 production as a function of distance was derived. The relation between distance and H_2O_2 production is not easily converted to a mathematical function, and is therefore stored as a vector.

It should be noted that the numerical simulations give virtually the same result as expected from using the G -value. The surface reaction is accounted for in the first volume element using the rate expression previously derived (Eq. (1)) [10]

$$r = k_{\text{H}_2\text{O}_2}[\text{H}_2\text{O}_2] \quad (1)$$

The rate constant, $k_{\text{H}_2\text{O}_2}$, for the reaction between H_2O_2 and UO_2 has been determined experimentally to $7.33 \times 10^{-8} \text{ m s}^{-1}$ [9]. Since spent nuclear fuel also contains

metallic ϵ -particles potentially capable of catalyzing H_2O_2 decomposition without leading to UO_2 oxidation, the rate constant for the H_2O_2 consumption was varied (between 7.33×10^{-8} and $7.33 \times 10^{-5} \text{ m s}^{-1}$) in the simulations. The variation is exaggerated (compared to the expected variation) to allow for a sensitivity analysis of the system. Diffusion between the volume elements is determined by the concentration gradient between two adjacent elements using Fick's first law (Eq. (2))

$$J = -D \frac{\partial C}{\partial x}. \quad (2)$$

The diffusion coefficient used for H_2O_2 was $10^{-9} \text{ m}^2 \text{ s}^{-1}$. The contributions from the above processes are added together and applied to the concentration vector to determine a new concentration vector for each time-step. To simulate the time evolution of the concentration profile an iterative process based on MATLAB was used.

3. Results and discussion

In Fig. 1, the H_2O_2 concentration profile for a mixed α - and β -radiation field corresponding to a fuel age of 100 years is given at 5, 10, 30, 60 and 120 s (surface reaction rate constant = $7.33 \times 10^{-5} \text{ m s}^{-1}$). The steady-state concentration (calculated using Eq. (3)) is also given in the figure,

$$[\text{H}_2\text{O}_2]_{s-s} = \frac{\overline{r_{\text{H}_2\text{O}_2}(\alpha)}\delta_{\text{max}}(\alpha) + \overline{r_{\text{H}_2\text{O}_2}(\beta)}\delta_{\text{max}}(\beta)}{k_{\text{H}_2\text{O}_2}}, \quad (3)$$

where $[\text{H}_2\text{O}_2]_{s-s}$ denotes the steady-state concentration of H_2O_2 , $\overline{r_{\text{H}_2\text{O}_2}}$ denotes the average radiolytic production rate for H_2O_2 , δ_{max} is the maximum range for α - or β -particles in water and $k_{\text{H}_2\text{O}_2}$ is the rate constant used for the surface reaction consuming H_2O_2 . Note that the steady-state expression is based on production and consumption of H_2O_2 per m^2 fuel surface.

As can be seen, the surface concentration fairly rapidly approaches the steady-state concentration also for mixed α - and β -fields. Consequently, the simplified steady-state approach for calculating the maximum dissolution rate can be employed also when the β -contribution is included. In Table 1, the maximum dissolution rates (based on α - and β -radiation) for spent fuel of ages 100–100 000 years are presented.

As can be seen, the maximum dissolution rate decreases with fuel age. The relative impact of β -radiation is also decreasing with fuel age.

As previously mentioned, the total rate constant for the surface reaction and thereby also the steady-state concentration is affected by the presence of ϵ -particles. However, even if the rate constant for the reaction between H_2O_2 and ϵ -particles is diffusion controlled a surface fraction of 1% ϵ -particles would only reduce the H_2O_2 steady-state concentration by a factor 3.9 [15]. In Fig. 2, the H_2O_2 concentration profiles corresponding to 90% of the steady-state surface concentration for the two highest surface reaction rate constants used in the simulations are plotted.

As can be seen, the surface concentrations as well as the shape of the concentration profiles differ considerably. However, it should be noted that only the two lowest surface reaction rate constants (7.33×10^{-8} and $7.33 \times 10^{-7} \text{ m s}^{-1}$) are relevant for dissolution of spent nuclear fuel. The reason for this is that, even though ϵ -particles in combination with H_2 could consume H_2O_2 with a diffusion controlled rate constant, the surface fraction of ϵ -particles under realistic conditions can only increase the rate constant for consumption of H_2O_2 by less than one order of magnitude.

Solutes reacting with H_2O_2 will also reduce the steady-state concentration. To elucidate the impact of such reactions we have performed a series of simulations where a homogeneous reaction consuming H_2O_2 is accounted for in each volume element.

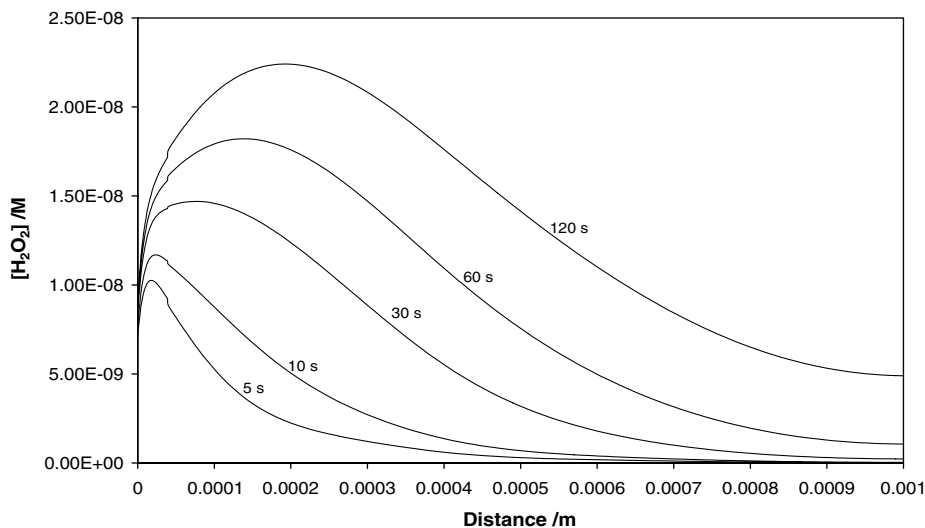


Fig. 1. H_2O_2 concentration profile as a function of reaction time.

Table 1
Maximum dissolution rates as a function of fuel age and burn-up

Age/years	38 MWd/kg		55 MWd/kg	
	$r_{\max}(\alpha)/\text{mol m}^{-2} \text{s}^{-1}$	$r_{\max}(\alpha + \beta)/\text{mol m}^{-2} \text{s}^{-1}$	$r_{\max}(\alpha)/\text{mol m}^{-2} \text{s}^{-1}$	$r_{\max}(\alpha + \beta)/\text{mol m}^{-2} \text{s}^{-1}$
100	3.65×10^{-10}	4.94×10^{-10}	5.27×10^{-10}	7.04×10^{-10}
1000	8.64×10^{-11}	8.72×10^{-11}	8.96×10^{-11}	9.68×10^{-11}
10000	1.65×10^{-11}	1.71×10^{-11}	1.70×10^{-11}	1.86×10^{-11}
100000	1.59×10^{-12}	1.79×10^{-12}	2.08×10^{-12}	2.41×10^{-12}

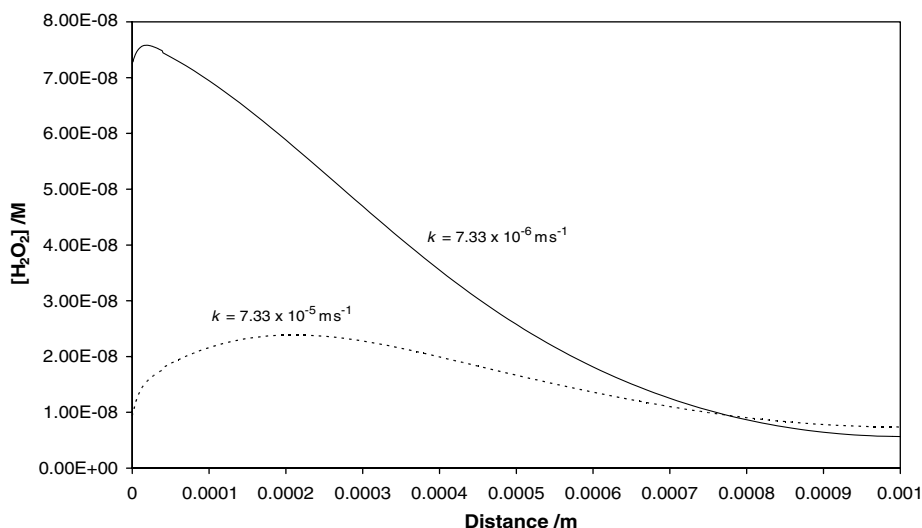


Fig. 2. H_2O_2 concentration profiles corresponding to steady-state conditions for two surface reaction rate constants.

In Fig. 3, the steady-state surface concentration of H_2O_2 is given as a function of pseudo first order rate constant, i.e. the second order rate constant multiplied by the concentration of the reactive solute ($k^* = k_{\text{hom}}[\text{solute}]$), for the homogeneous reaction.

As can be seen, the steady-state surface concentration decreases with increasing pseudo first order rate constant. The decrease is however not linearly related to the rate con-

stant for the process. The main reason for the non-linearity is the inhomogeneous production of H_2O_2 giving rise to concentration gradients. For higher homogeneous rate constants the bulk concentration of H_2O_2 approaches zero and the volume containing H_2O_2 decreases. Hence, the impact of increasing the rate constant further becomes lower. In a system with homogeneous production of H_2O_2 , e.g. γ -radiolysis, the decrease in steady-state concen-

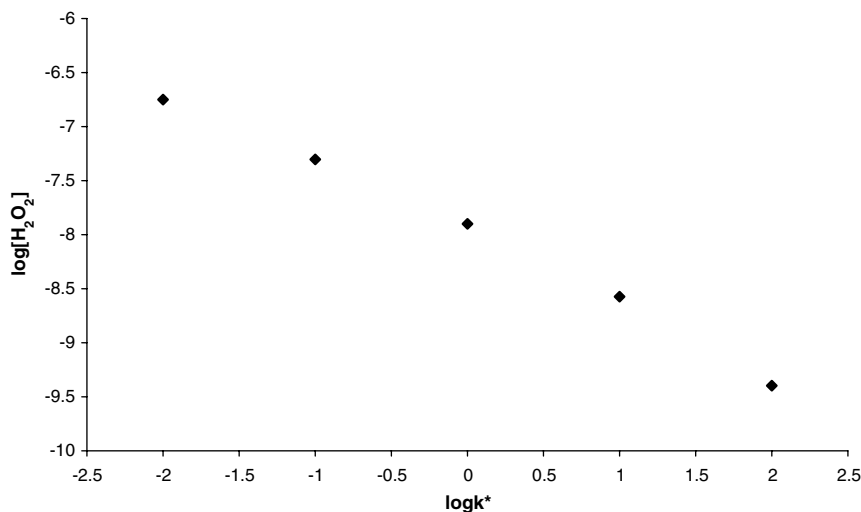


Fig. 3. The logarithm of the steady-state surface concentration of H_2O_2 plotted against the logarithm of the pseudo first order rate constant for bulk reactions consuming H_2O_2 .

Table 2

Steady-state H_2O_2 surface concentration as a function of surface reaction rate constant and homogeneous pseudo first order rate constant

Surface reaction rate constant (m s^{-1})	Homogeneous pseudo first order rate constant (s^{-1})						
	0	0.01	0.1	1	10	100	1000
7.33×10^{-8}	8.43×10^{-6}	1.78×10^{-7}	4.97×10^{-8}	1.26×10^{-8}	2.67×10^{-9}	4.01×10^{-10}	n.d.
7.33×10^{-7}	8.43×10^{-7}	n.d.	4.70×10^{-8}	1.26×10^{-8}	n.d.	n.d.	n.d.
7.33×10^{-6}	8.43×10^{-8}	n.d.	n.d.	1.05×10^{-8}	2.50×10^{-9}	3.79×10^{-10}	n.d.
7.33×10^{-5}	8.43×10^{-9}	n.d.	6.08×10^{-9}	3.93×10^{-9}	1.58×10^{-9}	3.35×10^{-10}	4.47×10^{-11}

tration will be linearly related to the pseudo first order rate constant of the homogeneous reaction.

To investigate the sensitivity of the system further, we have also performed a series of simulations where the rate constant for the surface reaction as well as the pseudo first order rate constant for the homogeneous reaction have been varied. The resulting steady-state surface concentrations of H_2O_2 are presented in Table 2.

As can be seen, the steady-state surface concentration is mainly determined by the homogeneous pseudo first order rate constant. However, for high surface reaction rate constants the steady-state surface concentrations are significantly lower for the lowest homogeneous pseudo first order rate constants. Hence, the system is governed by the surface reaction. As mentioned above, the rate constant for the reaction between H_2O_2 and the spent nuclear fuel surface is expected to be less than one order of magnitude higher than the rate constant for the reaction between H_2O_2 and UO_2 . Consequently, even for the low homogeneous pseudo first order rate constant, the steady-state surface concentration and thereby the rate of oxidation is governed by the bulk reaction. For this system, the relative steady-state surface concentration ($[\text{H}_2\text{O}_2]_{\text{s-s}}^*/[\text{H}_2\text{O}_2]_{\text{s-s}}$) as a function of the homogeneous pseudo first order rate constant is given by Eq. (4) (derived from Fig. 3). $[\text{H}_2\text{O}_2]_{\text{s-s}}^*$ is the surface concentration taking the bulk reaction into account and $[\text{H}_2\text{O}_2]_{\text{s-s}}$ is the surface concentration in the absence of bulk reactions consuming H_2O_2 ,

$$\log \frac{[\text{H}_2\text{O}_2]_{\text{s-s}}^*}{[\text{H}_2\text{O}_2]_{\text{s-s}}} = -0.66 \log k^* - 2.9 \quad (4)$$

It should be noted that Eq. (4) is independent of average dose rate. For aqueous solutions where several solutes display reactivity towards H_2O_2 , the pseudo first order rate constant, k^* , should be replaced by $\sum_i k_i [\text{solute}]_i$. The absolute steady-state surface concentration is given by the relative steady-state concentration multiplied by the maximum

steady-state concentration obtained from the dose rate according to Eq. (3). Hence, we now have a simple tool to calculate the maximum dissolution rate taking solution chemistry into account.

Acknowledgements

The Swedish Nuclear Fuel and Waste Management Company (SKB) and the Swedish Nuclear Power Inspectorate (SKI) are gratefully acknowledged for financial support.

References

- [1] D.W. Shoesmith, J. Nucl. Mater. 282 (2000) 1.
- [2] R.L. Segall, R.S.C. Smart, P.S. Turner, in: L.-C. Dufour (Ed.), Surface and Near-Surface Chemistry of Oxide Materials, Elsevier Science Publishers B. V., Amsterdam, 1988, p. 527.
- [3] J.W.T. Spinks, R.J. Woods, An Introduction to Radiation Chemistry, John Wiley, New York, 1964.
- [4] J.A.T. Smellie, M. Laaksoharju, P. Wikberg, J. Hydrol. 172 (1995) 147.
- [5] P. Wardman, J. Phys. Chem. Ref. Data 18 (1989) 1637.
- [6] R.E. Huie, C.L. Clifton, P. Neta, Rad. Phys. Chem. 38 (1991) 477.
- [7] I. Grenthe, F. Diego, F. Salvatore, G. Riccio, J. Chemical Society, Dalton Trans. 11 (1984) 2439.
- [8] E. Ekeröth, M. Jonsson, J. Nucl. Mater. 322 (2003) 242.
- [9] M.M. Hossain, E. Ekeröth, M. Jonsson, J. Nucl. Mater. 358 (2006) 202.
- [10] E. Ekeröth, O. Roth, M. Jonsson, J. Nucl. Mater. 355 (2006) 38.
- [11] F. Nielsen, M. Jonsson, J. Nucl. Mater. 359 (2006) 1.
- [12] F. Nielsen, K. Lundahl, M. Jonsson, J. Nucl. Mater., in press, doi:10.1016/j.jnucmat.2007.01.279.
- [13] R. Håkansson, Beräkningar av nuklidinnehåll, resteffekt, aktivitet samt doshastighet för utbränt kärnbränsle, SKB-R-99-74, 2000.
- [14] M.B. Carver, D.V. Hanley, K.R. Chaplin, MAKSIMA-CHEMIST a Program for Mass Action Kinetics Simulation by Automatic Chemical Equation Manipulation and Integration Using Stiff Techniques, Atomic Energy of Canada Limited – Chalk River Nuclear Laboratories, Ontario, 1979.
- [15] S. Nilsson, M. Jonsson, J. Nucl. Mater., in press, doi:10.1016/j.jnucmat.2007.03.040.